Biomaterials 34 (2013) 3547–3558

Contents lists available at SciVerse ScienceDirect

Biomaterials

journal homepage: www.elsevier.com/locate/biomaterials

Biological effects of cobalt-chromium nanoparticles and ions on dural fibroblasts and dural epithelial cells

Bharat Behl [a,b,1], Iraklis Papageorgiou [a,b,*,1], Christopher Brown [a,b], Richard Hall [a,c], Joanne L. Tipper [a,b], John Fisher [a,c], Eileen Ingham [a,b]

[a] Institute of Medical & Biological Engineering, University of Leeds, Leeds LS2 9JT, UK
[b] Institute of Molecular & Cellular Biology, Faculty of Biological Sciences, University of Leeds, Leeds LS2 9JT, UK
[c] School of Mechanical Engineering, University of Leeds, Leeds LS2 9JT, UK

ARTICLE INFO

Article history:
Received 4 December 2012
Accepted 4 January 2013
Available online 31 January 2013

Keywords:
Cobalt-chromium
Meninges
Cell viability
Nanoparticles
Cytokines
Oxidative stress

ABSTRACT

The introduction of metal-on-metal total disc replacements motivated studies to evaluate the effects of cobalt-chromium (CoCr) nanoparticles on cells of the dura mater. Porcine fibroblasts and epithelial cells isolated from the dura mater were cultured with clinically-relevant CoCr nanoparticles and the ions, generated by the particles over 24 h, at doses up to 121 μm^3per cell. Cell viability and production of proinflammatory cytokines was assessed over 4 days. The capacity of the particles to induce oxidative stress in the cells was evaluated at 24 h. The CoCr particles and their ions significantly reduced the viability of the dural epithelial cells in a dose-dependent manner but not the fibroblasts. Both cell types secreted IL-8 in response to particle exposure at doses of 60.5 μm^3 (epithelial cells) and 121 μm^3 (fibroblasts, epithelial cells) per cell. No significant release of IL-6 was observed in both cell types at any dose. Reactive oxygen species were induced in both cell types at 50 μm^3 per cell after 24 h exposure. The data suggested novel differences in the resistance of the dural epithelial cells and fibroblasts to CoCr nanoparticle/ion toxicity and demonstrated the inflammatory potential of the particles. The data contributes to a greater understanding of the potential biological consequences of the use of metal-on-metal total disc prostheses.

© 2013 Elsevier Ltd. All rights reserved.

1. Introduction

Degeneration of the intervertebral discs may lead in some individuals to a painful and disabling condition [1]. First line treatment generally includes non-invasive approaches such as rest, physiotherapy and analgesics. Patients are subjected to operative procedures when they do not respond to conservative treatment. A surgical procedure such as arthrodesis (spinal fusion) [2] is employed, however, its limitations include increased mechanical load at the adjacent and non-adjacent vertebrae and decrease in spine mobility that can lead to adjacent vertebrae degeneration [3]. For these reasons European surgical specialists on total hip and knee joint replacements started to experiment with total replacement of lumbar discs two decades ago, but the early operations led to some serious complications such as slippage of the artificial disc forward causing compression and damage to the aorta and the vena cava. It took nearly a decade for new designs to be developed and approved by the U.S. Food and Drug Administration following which more than 20,000 procedures were performed worldwide with more than 3000 in the United States alone [4]. This improved procedure of total disc replacement (TDR) has been developed with the objective of providing relief from pain and restoring motion between degenerated vertebrae [5]. New generation of artificial discs developed for TDR have gained increased popularity and preliminary studies have shown promising results [6,7]. Such prosthetic discs have the advantage of motion preservation and alleviation of adjacent segment degeneration [8]. The materials used in TDR have been adopted from experience in total hip arthroplasty. The two major types of TDR are the metal-on-polyethylene and metal-on-metal (MoM) implants [9]. The most extensively clinically utilised, studied and tested metal-on-polyethylene artificial discs are the Prodisc and the SB Charité total discs. The Flexicore and the Maverick total discs are two types of MoM artificial discs that can be used in TDR surgery [10].

* Corresponding author. Institute of Medical & Biological Engineering, University of Leeds, Leeds LS2 9JT, UK. Tel.: +44 1133435651.
E-mail address: I.papageorgiou@leeds.ac.uk (I. Papageorgiou).
[1] Behl and Papageorgiou are joint first authors.

0142-9612/$ – see front matter © 2013 Elsevier Ltd. All rights reserved.
http://dx.doi.org/10.1016/j.biomaterials.2013.01.023

However, there is currently very limited data (only case reports) available on the effectiveness and complications associated with spinal arthroplasty with virtually no long-term studies on the evaluation of the durability and sequelae of TDR surgeries. Case reports such as Berry *et al.* 2010 [11], Guyer *et al.* 2011 [12] and Cabraja *et al.* [13] revealed that MoM TDR can lead to the formation of granulomatous tissue with significant level of metalosis that can occlude or dislocate the surrounding arteries and veins and also cause spinal stenosis through infiltration of the spinal canal. This is of particular concern for MoM TDR, given the potential for toxicity of metal wear particles and the proximity to the spinal cord.

It is well established that prosthetic metal wear particles are in the nanometre size range [14,15]. The wear particles from simulators are of mean size smaller than 50 nm with round and irregular morphology [15] and similarly the mean size of the wear particles retrieved from periprosthetic tissues is also less than 50 nm (range: 6–834 nm) with round to oval shape and irregular boundaries [14]. These nanometre sized particles may disseminate to systemic regions away from the implant site such as local or distant lymph nodes, bone marrow, liver and spleen [16]. Significantly higher levels of cobalt and chromium ions have been reported in the serum of patients with MoM hips than those without [17] and this is a cause for concern as this may present a potential risk of carcinogenicity in humans and is directly associated with soft tissue changes [18]. Metal wear debris also has the capacity to induce host hypersensitivity [19,20]. Papageorgiou *et al.* [21], described the cytotoxic and genotoxic effects of CoCr nanoparticles on human fibroblasts *in vitro*. It has also been shown recently that CoCr nanoparticles and ions can cause DNA damage in cultured human fibroblasts even across cellular barriers [22] but this study had received considerable criticism [23].

There is an increasing concern regarding the development of periprosthetic soft tissue reactions in patients with some designs of MoM surface hip replacements [24]. These reports are beginning to raise questions about the long-term clinical implications of such pathologic observations associated with MoM prostheses, which are yet unknown. Similar cases have been presented in association with MoM TDR. Zeh *et al.* [25] examined 10 patients with Maverick lumbar disc replacements for an average of 5.6 years and reported the presence of CoCr ions in the serum. Cavanaugh *et al.* [26] published a case study in which a patient developed a delayed immune reaction to a MoM cervical artificial disc 9 months after surgery. In a recent case study, Berry *et al.* [11] were the first to report the formation of a large granuloma in a patient in response to metallic wear particles generated by a lumbar Maverick disc implantation. Moreover, Guyer *et al.* [12] presented a case study wherein four patients receiving MoM TDR developed periprosthetic necrosis and lymphocytic reactions resulting in failure of the TDR surgery. In one case report by Cabraja *et al.* [13], growth of this granulomatous tissue continued even after stabilization and reduction of the total disc arthroplasty device motion and so the clinicians were forced to remov the implant altogether.

It is possible that the wear particles produced in MoM TDRs can potentially interact with the dura mater (meninges). It is therefore imperative to determine the biological effects of these particles on the cells of the dura mater. The aim of this study was to investigate the biological effects of clinically relevant nanometre-sized CoCr wear particles on porcine dural cells extracted from the meninges that surround the spinal cord and are present in the immediate vicinity of artificial intervertebral discs implanted during TDR surgery. Porcine dural fibroblasts and epithelial cells were isolated and cultured with CoCr nanoparticles and the ions generated by the CoCr nanoparticles over 24 h at varying volumetric concentrations. Cellular responses were assessed using assays of cell viability, cytokine release and oxidative stress.

2. Materials and methods

2.1. Cobalt-chromium nanoparticle preparation and characterisation of size and sedimentation potential

Particles were generated in a 6 station pin-on-plate tribometer with water as the lubricant under a force of 80 N for 40 h. The pins and plates were manufactured from medical grade wrought CoCr alloy ASTM F1537 with smooth counterfaces (Ra: 0.01–0.02 μm). Wear particles were sterilised at 180 °C for 4 h and their mass determined by gravimetric analysis. The particles were then suspended in sterile water to yield a stock concentration of 1 $mg \cdot ml^{-1}$. A sample of the particle suspension was filtered through 0.015 μm polycarbonate filter membranes (Millipore Limited, UK). The isolated particles were characterized using field emission gun scanning electron microscopy (FEGSEM; FEI, The Netherlands) and Image Pro-Plus® imaging software. A total of 100 particles per image were analysed for 3 images.

In order to assess the particle sedimentation potential, CoCr-particle suspensions were prepared in dH_2O, DMEM (10% foetal bovine serum) and M199 medium (20% foetal bovine serum) (dural fibroablast and epithelial cell culture media). The particles were sonicated in a sonicating water bath (Grant Instruments Limited, UK) for 10 min and then the absorbance was measured at 204 nm over 2 s intervals for a period of 6 h using a M359 spectrophotometer (CamSpec, UK). The A/A_0 (A: Absorbance at time point; A_0: Absorbance at time = 0) was calculated for each time point and then plotted on a graph.

2.2. Ion release from the cobalt-chromium alloy nanoparticles

In order to measure the cobalt (Co), chromium (Cr) and molybdenum (Mo) ion concentrations that were released from the CoCr alloy nanoparticles over a period of time, two sets of clinically relevant particle suspensions were prepared at doses equivalent to 62, 6.2, 0.62, 0.062 $\mu g \cdot ml^{-1}$ in culture medium. One set of the particle doses was incubated at 37 °C in 5% (v/v) CO_2 in air for 1 day and the other set was incubated under the same conditions for 5 days. After incubation, the particle suspensions were centrifuged for 20 min at 3000 g and the supernatants containing the ions released from the particles were analysed. The Co and Cr ion levels in the supernatants were measured by graphite furnace atomic absorption spectroscopy whereas the Mo ion levels were measured by inductively coupled plasma mass spectroscopy.

2.3. Extraction of the dura mater

A UK Home Office protocol was employed to humanely sacrifice a female pig (65 kg) at the University of Leeds farm, which was then immediately transferred to the dissection table within few minutes of death. The skin covering the dorsal region was disinfected by swabbing with iodine solution and approximately 7–8 vertebrae from the thorax (T2–T10) were aseptically extracted. Following this, the intact extracted region of the vertebral column was transferred to the tissue culture laboratory under sterile conditions for further aseptic dissection. The dissected spinal cord with the attached meninges was then completely immersed in an antimicrobial solution (200 ml) containing Nystatin (100 $U.ml^{-1}$; Sigma–Aldrich, UK) and Gentamicin (50 $ng \cdot ml^{-1}$; Sigma–Aldrich, UK) in phosphate buffered saline (PBS; Sigma–Aldrich, UK) for 1 h at room temperature.

2.4. Cell isolation and culture

Samples of the fresh porcine dural membrane were dissected into ~1 cm^2 sections and then seeded in a 6-well culture plate (Fisher Scientific, UK). The tissue sections were cultured in M-199 medium (Lonza Biopharmaceuticals, UK) supplemented with 20% (v/v) foetal bovine serum (FBS; Lonza Biopharmaceuticals, UK), penicillin-streptomycin (50 $U.ml^{-1}$; Lonza Biopharmaceuticals, UK), L-glutamine (2 mM; Lonza Biopharmaceuticals, UK), sodium pyruvate (0.1 $mg \cdot ml^{-1}$; Sigma–Aldrich, UK), heparin (1 $U.ml^{-1}$; LEO Laboratories Limited, UK) and endothelial growth factor (0.015 $mg \cdot ml^{-1}$; Sigma–Aldrich, UK). The cells were allowed to outgrow for 7 days and culture expanded in supplemented M-199 medium by harvesting and transfers to 75 cm^2 culture flasks (Fisher Scientific, UK).

2.5. Separation of dural fibroblasts and epithelial cells

The cells were harvested after 7 days of growth using trypsin/EDTA (Lonza Biopharmaceuticals, UK) and centrifuged (200 g) and re-suspended in PBS supplemented with 0.1% (w/v) bovine serum albumin (BSA; Sigma–Aldrich, UK). The resulting cell suspension was centrifuged and re-suspended in PBS/BSA at a density of 2×10^6 $cells \cdot ml^{-1}$. The cells were separated using CD31 labelled magnetic Dynabeads® (endothelial cell-specific antibody, Invitrogen, UK). The Dynabeads (25 $\mu l \cdot ml^{-1}$) were incubated with the cell suspension at 2–8 °C with moderate rotation for 1 h, placed on a magnet (Invitrogen, UK) for 3 min. The flow-through was collected and the cells bound to the column were washed in PBS/BSA. This process was repeated twice. The unbound cells were also subjected to 3 steps of magnetic separation. The bound epithelial cells were collected by centrifugation (200 g) and re-suspended in supplemented M-199 medium while the unbound

fibroblasts were centrifuged (200 g) and re-suspended in supplemented Dulbecco's modified Eagle's medium (DMEM; Lonza Biopharmaceuticals, UK). Both cell types were seeded and expanded in 75 cm^2 culture flasks for 7 days and subjected to magnetic bead separation for a second time. Both the fibroblasts and the epithelial cells were maintained at 37 °C in 5% (v/v) CO_2 in air, trypsinised with trypsin/EDTA and subsequently passaged upon reaching 60–70% confluence.

2.6. Cell phenotyping

Porcine dural fibroblasts and epithelial cells were characterised by indirect immunofluorescence using primary antibodies against vimentin (mouse monoclonal, IgG2α; 1 : 100 dilution; Leica Biosystems, UK), tenascin (mouse monoclonal, TN2, IgG1k, 1 : 200 dilution; Novocastra Laboratories, UK), fibronectin (rabbit polyclonal, rabbit immunoglobulin fraction; 1 : 100 dilution; DakoCytomation, UK), actin α-smooth muscle (mouse monoclonal, 1A4, IgG2a; 1 : 200 dilution; Sigma–Aldrich, UK), collagen I (mouse monoclonal, 5D8-G9, IgG1k; 1 : 25 dilution; Millipore Limited, UK), collagen III (mouse monoclonal, IgG1; 1 : 25 dilution; Chemicon, UK), human CD31 (mouse monoclonal, 9G11, IgG1; 1 : 20 dilution; R & D systems, UK), desmoplakin I/II (mouse monoclonal, 2Q400, IgG1; 1 : 50 dilution; Abcam PLC, UK), E-cadherin (mouse monoclonal, 36B5, IgG1; 1 : 25 dilution; Vector Laboratories, UK), glucose transporter 1 (rabbit polyclonal, IgG; 1 : 50 dilution; Abcam PLC, UK), von Willebrand factor (rabbit anti-human polyclonal, rabbit immunoglobulin fraction; 1 : 100 dilution; DakoCytomation, UK), human fibroblasts/epithelial cells (mouse monoclonal, D7-FIB, IgG2a; 1 : 100 dilution; AbD Serotec, UK), porcine endothelial cells (mouse monoclonal, MIL11, IgE; 1 : 100 dilution; AbD Serotec, UK), desmin (mouse monoclonal, DE-R-11, IgG1; 1 : 200 dilution; Vector Laboratories, UK), smoothelin (mouse monoclonal, IgG1; 1 : 100 dilution; Millipore Limited, UK) and smooth muscle myosin heavy chain (mouse monoclonal, N1/5, IgG1; 1 : 100 dilution; Chemicon, UK).

Fluorescein isothiocyanate (FITC) labelled goat anti-mouse (1 : 500 dilution; Invitrogen, UK) and goat anti-rabbit (1 : 500 dilution; Invitrogen, UK) were used as secondary antibodies. Mouse IgG2α (1 : 500 dilution; DakoCytomation, UK) and rabbit anti-human immunoglobulin factor (1 : 500 dilution; DakoCytomation, UK) were used as antibody isotype controls. Antibodies were diluted in tris buffered saline (TBS; 0.15 M NaCl, 0.05 M tris, pH 7.6). Cells at a density of 4×10^4 cells ml^{-1} were applied (50 μl) to multispot slides (MP Biomedicals, UK) and incubated at 37 °C in 5% (v/v) CO_2 in air for 48 h. The slides were immersed in Dulbecco's phosphate buffer solution (DPBS) for 2 min and the cells fixed in ice-cold methanol : acetone (1 : 1; Genta Medical, UK) for 2 min, air dried for 30 min and rehydrated with distilled water for 2 min. The cells were treated with 0.05% (w/v) saponin (Sigma–Aldrich, UK) in TBS for 5 min. The cells were incubated with primary antibodies and isotype controls for 1 h at room temperature, washed in TBS-tween (TBS-T; 0.15 M NaCl, 0.05 M tris pH 7.6, 0.1% (v/v) Tween®-20 (Sigma–Aldrich, UK)) and then with TBS twice (5 min each). Cells were incubated with secondary antibodies for 30 min at room temperature, washed with TBS-T and TBS and counter stained with Hoechst dye (Sigma–Aldrich, UK) for 10 min, all in the dark. The slides were finally washed with TBS and distilled water (5 min each) and mounted in 1 : 9 (v/v) dabco : glycerol (Sigma–Aldrich, UK). The cells were viewed using a fluorescence microscope (BX51; Olympus, UK) and images were captured with a digital camera (XC50; Olympus, UK) and cell-B image processing software (Olympus, UK).

2.7. Treatment of cells with cobalt-chromium nanoparticles

The stock suspension of the CoCr nanoparticles (100 μl; 1 mg ml^{-1}) was diluted in appropriate culture medium (4.2 ml) to achieve a particle volume of 60.5 μm^3 per cell and subsequently 6.05 μm^3, 0.6 μm^3 and 0.06 μm^3 per cell by means of serial dilution. The highest dose of 121 μm^3 per cell was prepared by adding 200 μl of the particles stock to 4.2 ml of culture medium (47.6 μg ml^{-1}). The particles were sonicated in an ultrasonicator bath (Grant Instruments Limited, UK) for 10 min immediately before use. Cells were seeded into wells of 96-well flat bottomed plates (Fisher Scientific, UK) at a density of 5×10^3 cells per well (100 μl) and allowed to adhere for 3 h. The prepared particles were added (100 μl) and the cells incubated at 37 °C in 5% (v/v) CO_2 in air. Six replicates for each dose of CoCr nanoparticles were used in all experiments.

2.8. Treatment of cells with ions released from cobalt-chromium nanoparticles

In order to study the effect of metal ions that were released from the CoCr nanoparticles, the same particle concentrations as described above were prepared (47.6, 23.8, 2.38, 0.238 and 0.0238 $\mu g \cdot ml^{-1}$). After 24 h incubation of the particles in culture medium at 37 °C in 5% (v/v) CO_2 in air, the particle suspensions were centrifuged for 20 min at 3000 g and the supernatants containing the ions released from the particles were collected and stored at −20 °C until needed.

2.9. Determination of the effects of cobalt-chromium nanoparticles and their released ions on cell viability

The effect of the particles on the viability of the porcine fibroblasts and epithelial cells was evaluated using the adenosine triphosphate-lite™ (ATP-lite™; PerkinElmer Life Sciences, UK) assay kit according to the manufacturer's instructions. The cells were exposed to CoCr nanoparticles at volumes of 121 μm^3, 60.5 μm^3, 6.05 μm^3, 0.6 μm^3 and 0.06 μm^3 per cell. The cells were also exposed to metal ions released over a period of 24 h incubation from the particle concentrations by adding the conditioned medium produced as described above. ATP levels were determined at 24 h intervals over a period of 4 days. Cells only were used as a negative control and camptothecin (2 $\mu g \cdot ml^{-1}$; Sigma–Aldrich, UK) was used as a positive control. The luminescence of ATP was measured in counts per second (CPS) using the Topcount® microplate scintillation and luminescence counter (Packard Bioscience, UK).

2.10. Determination of the effects of cobalt-chromium nanoparticles on cytokine secretion

The porcine dural fibroblasts and epithelial cells were cultured with CoCr nanoparticles at a range of volumes (121 μm^3–0.06 μm^3 per cell). Culture supernatants were harvested at 24 h intervals over a period of 4 days and stored at −20 °C until assayed. Cells only were used as a negative control and lipopolysaccharide (LPS; 2 $\mu g \cdot ml^{-1}$; Sigma–Aldrich, UK) was used as a positive control. The levels of IL-6 and IL-8 produced by the cells were evaluated using commercial sandwich enzyme-linked immunosorbent assay (ELISA) kits (R & D systems, UK) following the manufacturer's instructions. Results are presented as the specific activity which is the concentration of cytokine (in $pg \cdot ml^{-1}$) divided by the CPS determined by the ATP-lite™ assay.

2.11. Determination of the effects of cobalt-chromium nanoparticles on intra-cellular oxidative stress

Porcine dural fibroblasts and epithelial cells were cultured on multispot slides (8-spot; MP Biomedicals, UK) with CoCr nanoparticles at a particle volume of 50 μm^3 per cell. Cells only as well as particles only were used as negative controls. Oxidative stress was assessed using 5 - (and - 6) - carboxy - 2′, 7′- dichlorodihydrofluorescein

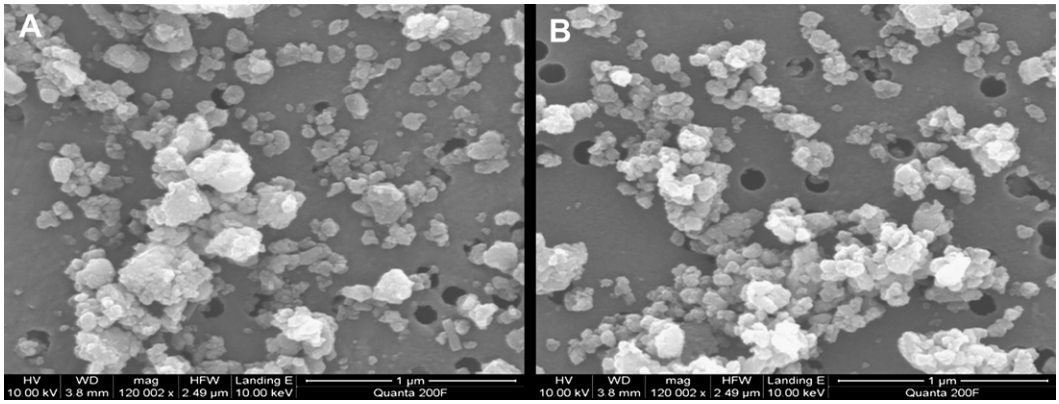

Fig. 1. FEGSEM images of isolated CoCr nanoparticles. (A) and (B) CoCr nanoparticles were generated using a 6-station pin-on-plate tribometer with distilled water as the lubricant and subsequently isolated by filtration onto a 0.015 μm polycarbonate filter membrane. Images of the particles were obtained by field emission scanning electron microscopy at 120002× magnification. The particles visualised were round, oval or irregular in morphology.

diacetate (carboxy-H_2DCFDA; Invitrogen, UK) after a 24 h exposure of the cells to the particles. Intra-cellular reactive oxygen species (ROS) levels were detected by fluorescence microscopy and cell-B image acquisition program using the Image-iT™ LIVE Green Reactive Oxygen Species Detection Kit (Invitrogen, UK). Intra-cellular ROS levels were estimated by segregating the fluorescence intensity of 100 individual cells into four categories which were no fluorescence, weak fluorescence, strong fluorescence and very strong fluorescence. The procedure was carried out in duplicate (2 spots) in accordance with the protocol supplied by the manufacturer.

2.12. Statistical analysis

Data is presented as the mean ± 95% confidence limits. Data was analysed by one-way analysis of variance (ANOVA) and individual differences between group means were determined using the post-hoc T-method to calculate the minimum significant difference (MSD; $p < 0.05$).

3. Results

3.1. Characterisation of cobalt-chromium nanoparticles

The CoCr wear particles were generated using a 6-station pin-on-plate tribometer and isolated by filtration onto a 0.015 μm polycarbonate filter membrane. Images of the particles were obtained using FEGSEM. The CoCr nanoparticles had formed aggregates and appeared mostly round, oval or irregular shaped in morphology (Fig. 1). The nanoparticles had a mode size of 40–49 nm although a high frequency of particles in the size range of 30–39 nm and 50–59 nm was also observed (Fig. 2A). The mode area of the nanoparticles was found to be 50–59 nm (Fig. 2B).

The sedimentation rate of CoCr nanoparticles in dH_2O increased as the particle concentration increased. However, after 4–5 h the majority of the particles at all 3 doses (0.05, 0.5 and 1 mg·ml^{-1}) had already fully sedimented (Fig. 3A). At a nanoparticle concentration of 0.5 mg ml^{-1}, the sedimentation rate of the particles in both media (DMEM and M199) was similar to that observed in dH_2O (Fig. 3B). However, for the two culture media, particles sedimented at a slower rate in M199 medium compared to DMEM. The only difference between the two complete media types was the difference in FBS content .i.e. and 10% (v/v) in DMEM and 20% (v/v) in m199medium. At around 6 h the majority of the particles for both types of media had fully sedimented as seen in Fig. 3B.

3.2. Ion release from cobalt-chromium alloy nanoparticles

The concentration of Co, Cr and Mo ions released by the particle suspensions after both 1 and 5 days of incubation in culture medium is shown in Table 1. At 1 day of incubation there was a release of Co, Cr and Mo ions from all particle concentrations, but the amount of ions released was in the ng per ml scale even at the highest particle concentration of 62 μg·ml^{-1} (Co:368, Cr:433 and Mo: 291 ng ml^{-1}). The concentration of metal ions released at 1 and 5 days also differed. The Co and Mo ion release from the 62 and 6.2 μg per ml particle solutions at 5 days had decreased by approximately 11% in comparison with the corresponding solutions incubated for 1 day. However, there was a decrease of approximately 33% in Cr concentrations in the 62 and 6.2 μg per ml particle solutions incubated for 5 days in comparison with the corresponding particle solutions incubated for 1 day. For this reason, incubation of the particles in medium for 1 day was chosen to assess the biological effects of the metal ions released from the CoCr nanoparticles.

3.3. Characterisation of dural meningeal cell lines

The outgrowth of cells from the porcine dural tissue explants after 7 days exhibited a mixture of fibroblasts and epithelial cells. After subjecting the cells to magnetic bead separation, they were distinctly separated into fibroblast and epithelial cell morphologies (images not shown).

A wide range of different antibodies was employed to extensively phenotype the two cell types (Table 2). Both dural fibroblasts and epithelial cells were stained positive for vimentin (Fig. 4),

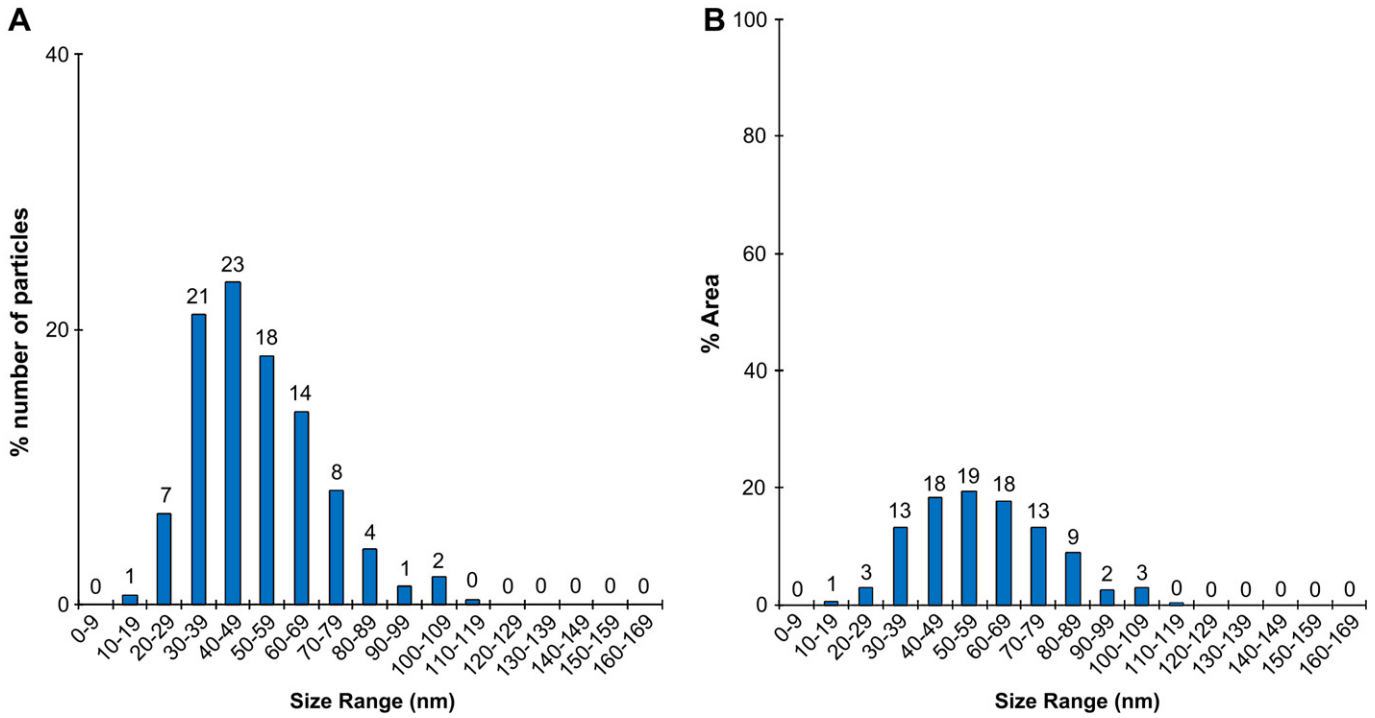

Fig. 2. Size and area frequency of CoCr nanoparticles. The size (A) and area (B) distribution of the CoCr nanoparticles was calculated from the FEGSEM images using the Image pro-Plus imaging software. The mean size and area if the particles was 40–49 nm and 50–59 nm respectively; 100 particles were measured using 3 replicate sample images.

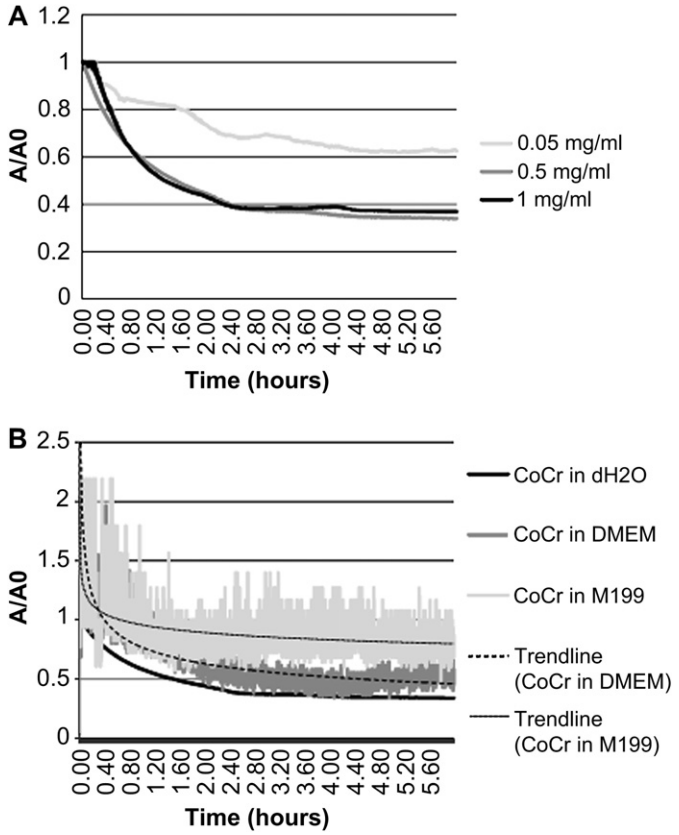

Fig. 3. Sedimentation curves for CoCr nanoparticles over a period of 6 h. (A) The sedimentation rate of 3 different concentrations of nanoparticles in dH2O was assessed. (B) The sedimentation rate of 1 mg ml^{-1} nanoparticles in 3 different media: dH2O, DMEM and M199 was measured. In each case the absorption value at each time point (A) was divided by the absorption value at time = 0 (A_0) and plotted against time.

tenascin, fibronectin, actin and collagen I and III. By contrast, only the epithelial cells were stained positively for von Willebrand factor (Fig. 5) and CD31 and hence they demonstrated typical endothelial cell-like characteristics. In addition, von Willebrand factor was found to be localised within the cytoplasm while CD31 was confined towards the periphery of the cells (cell membrane), giving them a mosaic appearance at 100× magnification. The epithelial cells, unlike the fibroblasts, also stained positive for E-cadherin.

The dural fibroblasts and epithelial cells were also tested for the expression of desmoplakin I/II and glucose transporter 1 (GLUT1) to determine any possibility of barrier formation. Both cell types were shown to express GLUT1 but only the epithelial cells stained positive for desmoplakin I/II, particularly in highly confluent regions.

Table 1
Mean concentration of cobalt, chromium and molybdenum ions release in medium after incubation for 1 and 5 days. All particle suspensions were prepared in duplicate. Cobalt and chromium levels were measured by graphite furnace atomic absorption spectroscopy and the molybdenum levels were assessed by inductively coupled plasma mass spectroscopy. The ion concentrations released into solution are expressed in ng ml^{-1}.

	Incubation period (days)	1			5		
		Co	Cr	Mo	Co	Cr	Mo
Particle suspensions used ($\mu g \cdot ml^{-1}$)	62	368	433	291	324	292	263
	6.2	51	61	34	45	40	30
	0.62	7.5	15	5.2	6.5	5.6	5.5
	0.062	1.0	8.3	2.7	0.8	1.0	1.4

Table 2
Characterisation of porcine dural fibroblasts and epithelial cells as determined by expression of specific proteins using indirect immunofluorescence labelling. Primary smooth muscle cells were used as the positive control for contamination by smooth muscle cells. (+ve: Positive signal, ve: No signal, —:Not tested).

Antibody target	Dural fibroblasts	Dural epithelial cells	Primary smooth muscle cells
Vimentin	+ve	+ve	———
Tenascin	+ve	+ve	———
Fibronectin	+ve	+ve	———
Actin	+ve	+ve	+ve
Collagen I	+ve	+ve	———
Collagen III	+ve	+ve	———
von Willebrand factor	-ve	+ve	-ve
CD31	-ve	+ve	-ve
E-cadherin	-ve	+ve	———
Desmoplakin	-ve	+ve	-ve
GLUT1	+ve	+ve	+ve
Human fibroblasts/epithelial cells	-ve	-ve	———
Porcine endothelial cells	-ve	-ve	-ve
Desmin	-ve	-ve	+ve
Smoothelin	-ve	-ve	+ve
Smooth muscle myosin heavy chain	-ve	-ve	+ve

Finally, both dural fibroblasts and epithelial cells were treated with antibodies against desmin, smoothelin and smooth muscle myosin heavy chain to confirm the absence of any contamination from smooth muscle cells. Neither the fibroblasts nor the epithelial displayed expression of any of the smooth cell specific markers (Table 2). However, smooth muscle cells stained positively using these antibodies thereby demonstrating their specificity.

3.4. Effects of cobalt-chromium nanoparticles and their released metal ions on the viability of dural fibroblasts and epithelial cells

The porcine dural fibroblasts (Fig. 6A) and epithelial cells (Fig. 6B) were cultured with CoCr nanoparticles at volumes of 121 μm^3, 60.5 μm^3, 6.05 μm^3, 0.6 μm^3 and 0.06 μm^3 per cell. Additionally, the porcine dural fibroblasts (Fig. 6C) and epithelial cells (Fig. 6D) were cultured with media containing metal ions released from the CoCr nanoparticles over a period of 24 h incubation. The effects of the particles and ions on the cells were evaluated separately using the ATP-lite™ assay over a period of 4 days. As shown in Fig. 6A, the CoCr nanoparticles had no effect on the viability of the dural fibroblasts as compared to the cells only negative control. In contrast, the CoCr nanoparticles caused a dose-dependent decrease in the intra-cellular ATP levels of the epithelial cells as compared to the cells only negative control (Fig. 6B). A significant reduction in cell viability ($p < 0.05$) was observed for the cells cultured with particle volumes of 6.05 μm^3, 60.5 μm^3 and 121 μm^3 per cell. This effect was evident on day 1 of culture and persisted until day 4.

Similar effects on cell viability were observed when the cells were treated with metal ions released from the metal particles. As shown in Fig. 6C, the metal ions had no significant effect on the viability of the dural fibroblasts. However, the metal ions caused a significant decrease in cell viability ($p < 0.05$) of the epithelial cells at the highest dose (121 μm^3 per cell, 47.6 $\mu g \cdot ml^{-1}$) and this was evident on day 3 and 4.

3.5. Induction of proinflammatory cytokines by cobalt-chromium nanoparticles

The culture supernatants of particle-treated cells were obtained and analysed for proinflammatory cytokine (IL-6 & IL-8) secretion over a period of 4 days. The CoCr nanoparticles failed to stimulate

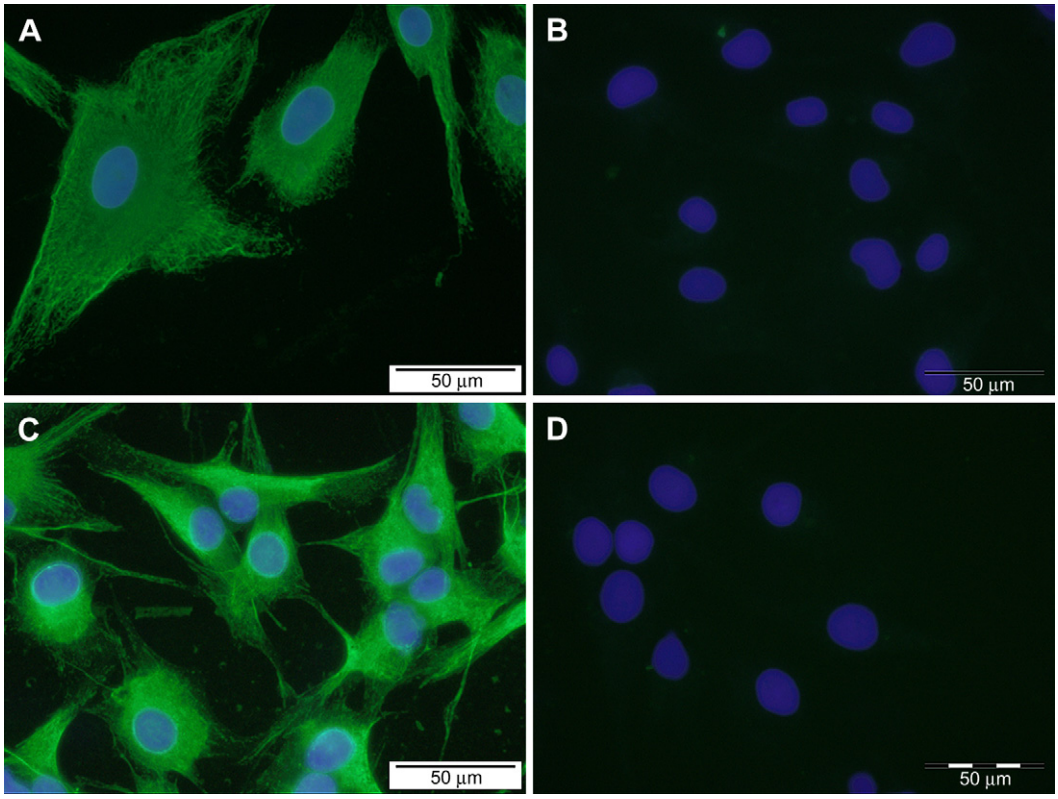

Fig. 4. Fluorescence microscopy images of porcine dural fibroblasts and dural epithelial cells treated with primary antibody to vimentin and isotype control. Fibroblasts (A, B) and epithelial cells (C, D) were subjected to immunofluorescence analysis and images obtained by fluorescence microscopy at 400× magnification. (A, C) Both cell types were stained positive for vimentin (green) using mouse monoclonal primary antibody. (B, D) No staining of vimentin was observed when the cells were treated with mouse IgG2α (isotype). The nuclei of the cells appeared blue as a result of counterstaining with the Hoechst stain.

IL-8 secretion by the fibroblasts at doses up to 60.5 μm^3 per cell (Fig. 7A). For the epithelial cells, no significant increase in the production of IL-8 was detected below a dose of 6.05 μm^3 per cell at all time points (Fig. 7B). However, a significant increase in IL-8 production ($p < 0.05$) was observed when the cells were cultured with the CoCr nanoparticles at higher doses of 60.5 μm^3 and 121 μm^3 per cell (Fig. 7B). These effects were observed on day 1 through day 4 of culture. Neither the fibroblasts nor the epithelial cells secreted IL-6 in response to the CoCr nanoparticles or LPS (data not shown).

3.6. Induction of intra-cellular oxidative stress by cobalt-chromium nanoparticles

The induction of oxidative stress in the dural fibroblasts and epithelial cells was determined following exposure of the cells to CoCr nanoparticles at a volume of 50 μm^3 per cell. Intra-cellular ROS levels were detected after 24 h using carboxy-H_2DCFDA. Increased levels of intra-cellular ROS were observed in the fibroblasts cultured with CoCr nanoparticles when compared to the cells only negative control (Fig. 8A,B&C). Upon evaluation of the fluorescence intensity from 100 individual cells, 50% of the particle-treated cells were shown to have emitted very strong fluorescence while 40% of the cells exhibited a relatively strong signal and approximately 10% of the particle-exposed cells displayed weak fluorescence (Table 3). On the other hand, 72% of the untreated cells exhibited no fluorescence signal whereas 23% emitted a relatively weak signal and 5% of the cells showed strong fluorescence (Table 3). A similar effect was observed with epithelial cells in which intra-cellular ROS levels were also higher in comparison to the cells only negative control (Fig. 8D,E&F). Upon evaluation of the fluorescence intensity from 100 individual cells, 62% of the particle-treated cells were shown to have emitted very strong fluorescence while 25% of the cells exhibited a relatively strong signal and approximately 13% of the particle-exposed cells displayed weak fluorescence (Table 3). For the untreated cells, 64% exhibited no fluorescence signal whereas 28% emitted a relatively weak signal and 8% of the cells showed strong fluorescence (Table 3). Also, the particles only (negative control) were not able to induce by themselves any ROS-related signal (images were not shown).

4. Discussion

Total hip arthroplasty was originally conceived by Sir John Charnley as a procedure for elderly patients with low activity levels [27]. However, the indications and projections for joint arthroplasty have expanded to include both younger (less than 65 years old) and more active patients [28]. These higher-demand patients have expectations and intentions to return to prior activity levels that challenge surgical techniques and implant design technology [29]. This lead to an increased requirement for the implantation of orthopaedic metal-on-metal hip prostheses in younger individuals which has raised substantial concerns about their long term potential risks (adverse soft tissue reactions, high blood metal ions) and health implications [30]. The use of MoM prostheses in TDR relies on the same basic principles and materials involved in the development of similar implants for total hip replacements.

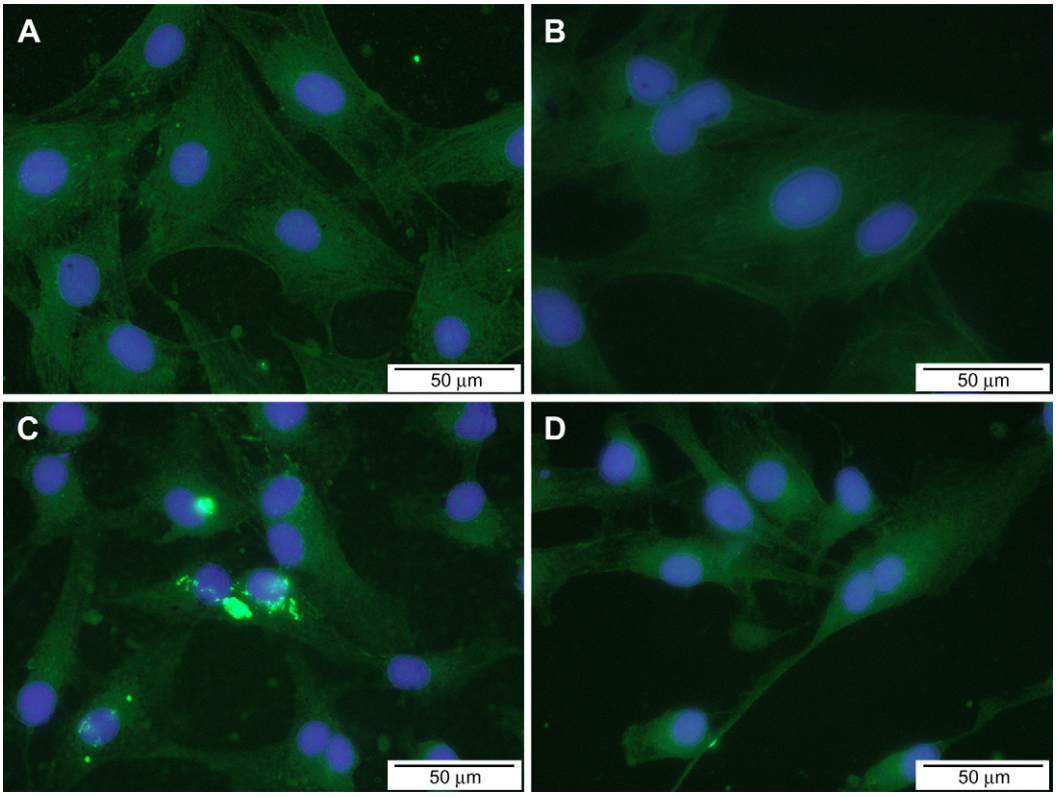

Fig. 5. Fluorescence microscopy images of porcine dural fibroblasts and dural epithelial cells treated with primary antibody to von Willebrand factor and isotype control. Fibroblasts (A, B) and epithelial cells (C, D) were subjected to immunofluorescence analysis and images obtained by fluorescence microscopy at 400× magnification. Epithelial cells (A) were stained positive (bright green) whereas fibroblasts (B) appeared negative (absence of bright green staining) for von Willebrand factor using rabbit polyclonal primary antibody. (C, D) No staining of von Willebrand factor was observed when the cells were treated with rabbit immunoglobulin factor (isotype). The nuclei of the cells appeared blue as a result of counterstaining with the Hoechst stain.

However, little attention has been paid to the adverse biological effects of intervertebral disc prostheses. There is therefore, a dearth of information on the biological reactivity of wear debris released from spinal implants and hence much of the knowledge about metal wear particles from hip arthroplasty has been extrapolated to the spinal arthroplasty environment. The aim of this *in vitro* study was to investigate the potential biological effects of prosthetic CoCr nanoparticles on porcine dural fibroblasts and epithelial cells that form an integral part of the spinal meninges.

Characterisation of metal wear debris has more commonly been associated with total joint replacement than TDR and hence there is a lack of information about the analysis of particles originating from TDRs that are either failed or acquired during a post-mortem. However, particles generated from TDRs are likely to be similar in size, shape and topographic characteristics to those generated from total joint replacements due to similar articulating surfaces and tribological interactions. In a review, Hallab [31]. has shown that the wear rate (volume) and particle size in metal-on-metal bearings is similar between TDR and total hip arthroplasties. The CoCr wear particles used in this study were shown to have a size distribution of 10–119 nm with a mode size of 40–49 nm. These results are consistent with previous findings of nanoparticles generated by metal-on-metal bearings [32,33]. The morphology of the CoCr nanoparticles was either round, oval or irregular shaped with the formation of aggregates. Sonication was employed for short period of time (for 10 min) in order to break these nanoparticle aggregates and avoid re-agglomeration of the nanoparticles that can occur at longer duration of sonication (more than 30 min) [34]. The chance that re-agglomeration can occur after the lapse of the sonication and during treatment of the cells [35,36] is unavoidable and probably occurs during the *in vivo* production and the dispersal of the CoCr nanoparticles to the surrounding tissues.

Metal ions were released from these nanoparticles during in the first 24 h of incubation in culture media. However, this ion release did not increase as the incubation time progressed (after 5 days). These results are consistent with a previous study by Papageorgiou *et al.* [21], which demonstrated that Co and Cr ion release from CoCr alloy micron size particles was maximum at 24 h incubation and did not significantly increase at 48 h. The authors suggested that this was due to a passive film formation that restricted any further corrosion and ion release.

Sedimentation of the CoCr nanoparticles was concentration dependant as well as dependent upon the medium. Sedimentation was faster at higher concentrations. This indicated that the particle concentration affected the rate and degree of agglomeration by enhancing the rate of direct particle to particle association [37]. However, irrespective of the particle concentration the majority of the particles were fully sedimented prior to 6 h time point.

Particles dispersed in high concentration FBS-medium (20%) (M199) had a slower sedimentation rate compared to when dispersed in low concentration FBS-medium (10%) (DMEM). The colloidal stability of the CoCr nanoparticles increased as the concentration of FBS increased. According to Allouni *et al.* [37], protein adsorption to the surface of the particles plays a decisive role in governing disposition. Albumin which is the dominant protein in FBS, can bind to the surface of nanoparticles and thus lead to stable colloidal dispersion of the nanoparticles possibly by a steric stabilisation mechanism [38].

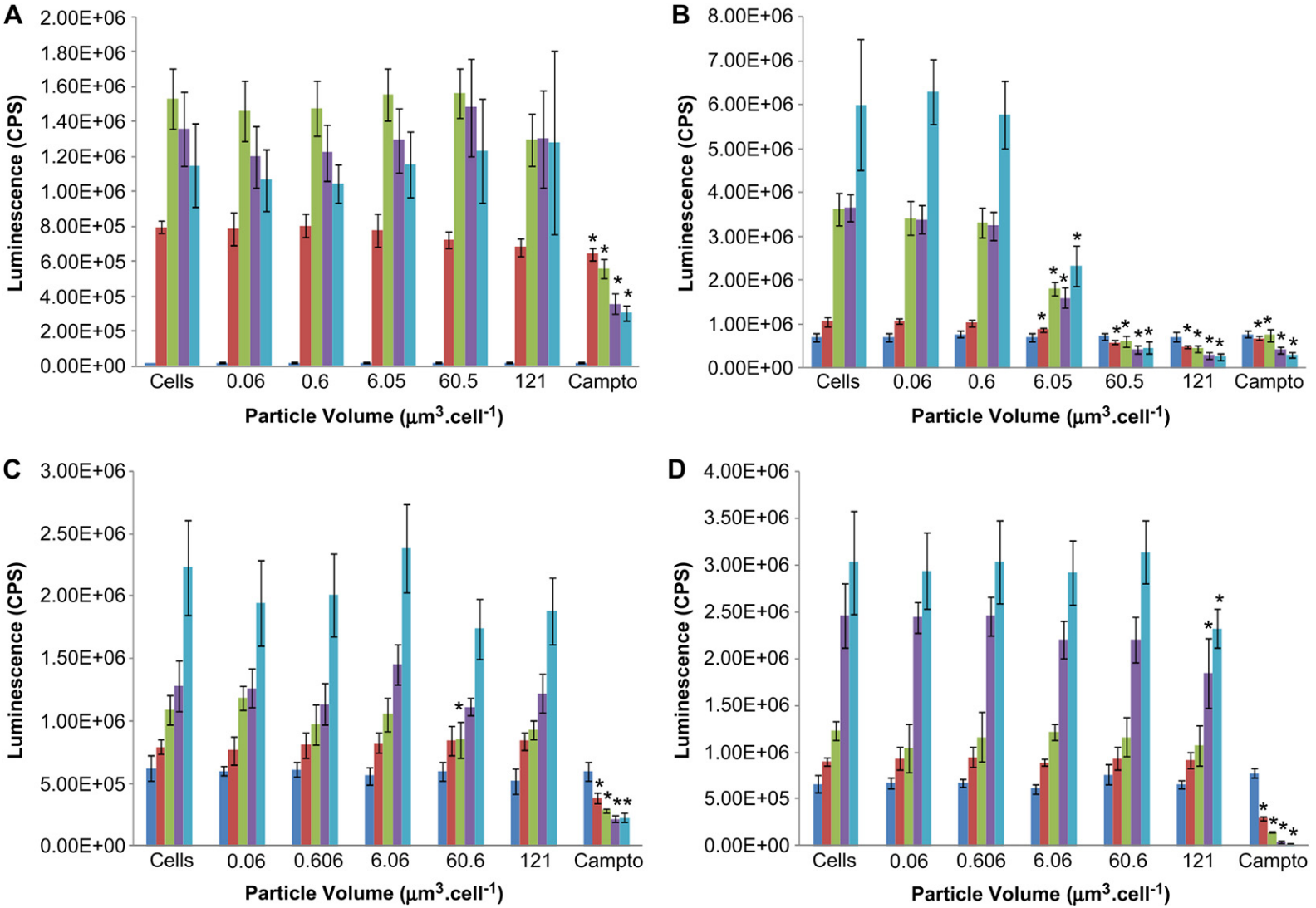

Fig. 6. Effects of CoCr nanoparticles and metal ions on viability of porcine dural fibroblasts and dural epithelial cells. Fibroblasts (A, C) and epithelial cells (B, D) were separately cultured with various volumes of CoCr nanoparticles (A, B) and their released metal ions (C, D) for up to 4 days. Cells only were used as the negative control and camptothecin (2 μg ml^{-1}) as the positive control for cell death. Cell viability was determined using the ATP-lite™ assay at 24 h intervals. Data is expressed as the mean ($n = 6$) ± 95% confidence limits. Cell viability data was analysed using one-way ANOVA test and MSD calculated using the *T*-test. A statistical decrease ($p < 0.05$) in cell viability compared to the cells only control, at each time point, is indicated by an asterisk (*). The colour key indicates the following days: ■, day 0; ■, day 1; ■, day 2; ■, day 3; ■, day 4.

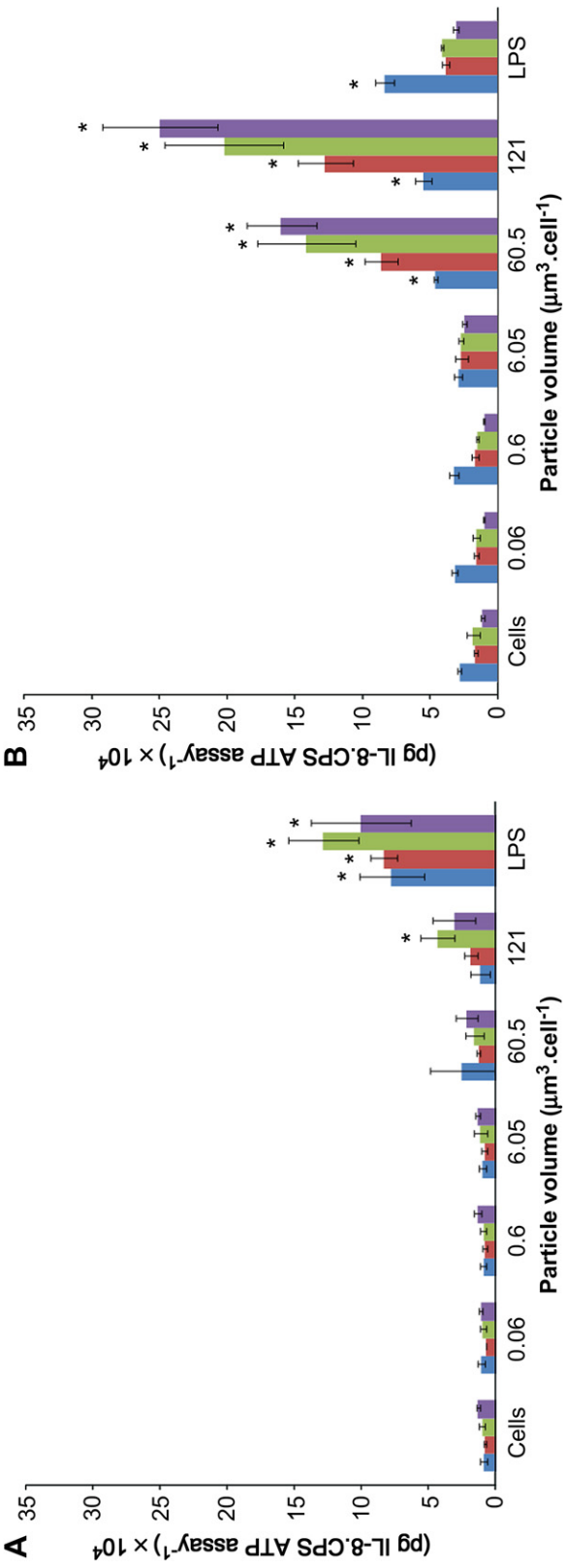

Fig. 7. Specific activity of IL-8 released from porcine dural fibroblasts and dural epithelial cells exposed to CoCr nanoparticles. Fibroblasts (A) and epithelial cells (B) were cultured with various volumes of CoCr nanoparticles up to 4 days. Cells only were used as the negative control and LPS (2 μg ml^{-1}) as the positive control. Culture supernatants were subjected to cytokine analysis at regular intervals. Data is expressed as the mean ($n = 3$) ± 95% confidence limits. Cytokine release data was analysed using the one-way ANOVA test and the MSD calculated using the *T*-test. A statistical increase ($p < 0.05$) in cytokine release compared to the cells only control, at each time point, is indicated by an asterisk (*).The colour key indicates the following days: ■, day 1; ■ day 2; ■, day 3; ■, day 4.

The reason the pig was chosen as a model was due to the fact that it shares anatomical and physiological characteristics to humans [39]. Additionally, the pig immune system has been found to closely resemble that of humans for more than 80% of parameters examined and may therefore be used in the study of human disease processes [40]. Also, the reason that primary cells were used instead of established cell lines was due to the fact that cell lines could lose some of their physiological as well as biochemical characteristics as seen in many studies [41–43].

The porcine dural fibroblasts and epithelial cells used in this study were first characterised before investigating their response to CoCr nanoparticles. This was accomplished by examining the expression of specific markers in the two cells lines using indirect immunofluorescence. Both the fibroblasts and the epithelial cells were strongly stained for vimentin, which is an intermediate filament protein and is known to be expressed in cells of the mesenchymal origin [44]. The epithelial cells only, expressed E-cadherin, which is involved in calcium dependent cell–cell adhesion [45] and desmoplakin I/II, which are abundant components of desmosomes [46]. The dural epithelial cells were positively stained for desmoplakin I/II particularly in regions of high confluence, which further supports their role in maintaining tight junction barriers in the meninges [47] to avoid undesirable foreign invasion. Hence, the dural epithelial cells predominantly exhibited typical epithelial cell-like characteristics.

Additionally, both dural epithelial and fibroblast cells were shown to ubiquitously express GLUT1, which is an integral membrane protein that functions as a facilitative glucose transporter in mammalian cells. This indicated that both cell types may have utilised this transporter to meet their energy needs. GLUT1 has been found to be expressed abundantly in fibroblasts and endothelial cells and may also serve as a means of glucose transport across the blood–brain barrier [48]. Immunocytochemical analysis also revealed that the dural epithelial cells uniquely stained positive for CD31 and von Willebrand factor, which are established markers for endothelial cells [49]. Both the dural fibroblasts and epithelial cells were also found to be free from smooth muscle contamination as indicated by an absence of staining by antibodies against desmin, smoothelin and smooth muscle myosin heavy chain. Thus, both the cell types were successfully characterised and distinguished, based on differences in their phenotypes.

CoCr nanoparticles have been found to be cytotoxic to wide variety of cells including those present in the periprosthetic environment [50]. Necrosis and abnormal soft tissue reactions called pseudotumours have also been observed in periprosthetic tissues associated with MoM prostheses [51]. The *in vitro* cytotoxic effects of CoCr nanoparticles on periprosthetic dural cells have not been previously investigated. Porcine dural fibroblasts and epithelial cells were cultured with the particles for 4 days at volumes ranging from 0.06 μm^3 to 121 μm^3 per cell. The CoCr nanoparticles were shown to be cytotoxic to the dural epithelial cells in comparison to the dural fibroblasts. The particles significantly reduced the viability of the epithelial cells from day 1 up to day 4 of culture at doses of 6.05 μm^3 and above. Conversely, there was no significant reduction in the viability of the dural fibroblasts at all the particle doses and time points studied. In their study, Papageorgiou *et al.* [21] demonstrated that CoCr nanoparticles were cytotoxic to human dermal fibroblasts at doses as low as 5 μm^3 per cell. However in this study, no significant reduction in the viability of the porcine dural fibroblasts was observed at particle doses up to 121 μm^3 per cell. This discrepancy may have been due to a difference in the tissue of origin of the fibroblasts, an inter-species variation or due to the particles being less biologically reactive. Moreover, the difference in toxicity of the CoCr nanoparticles for the two cell types could not be explained by the fact that the nanoparticles

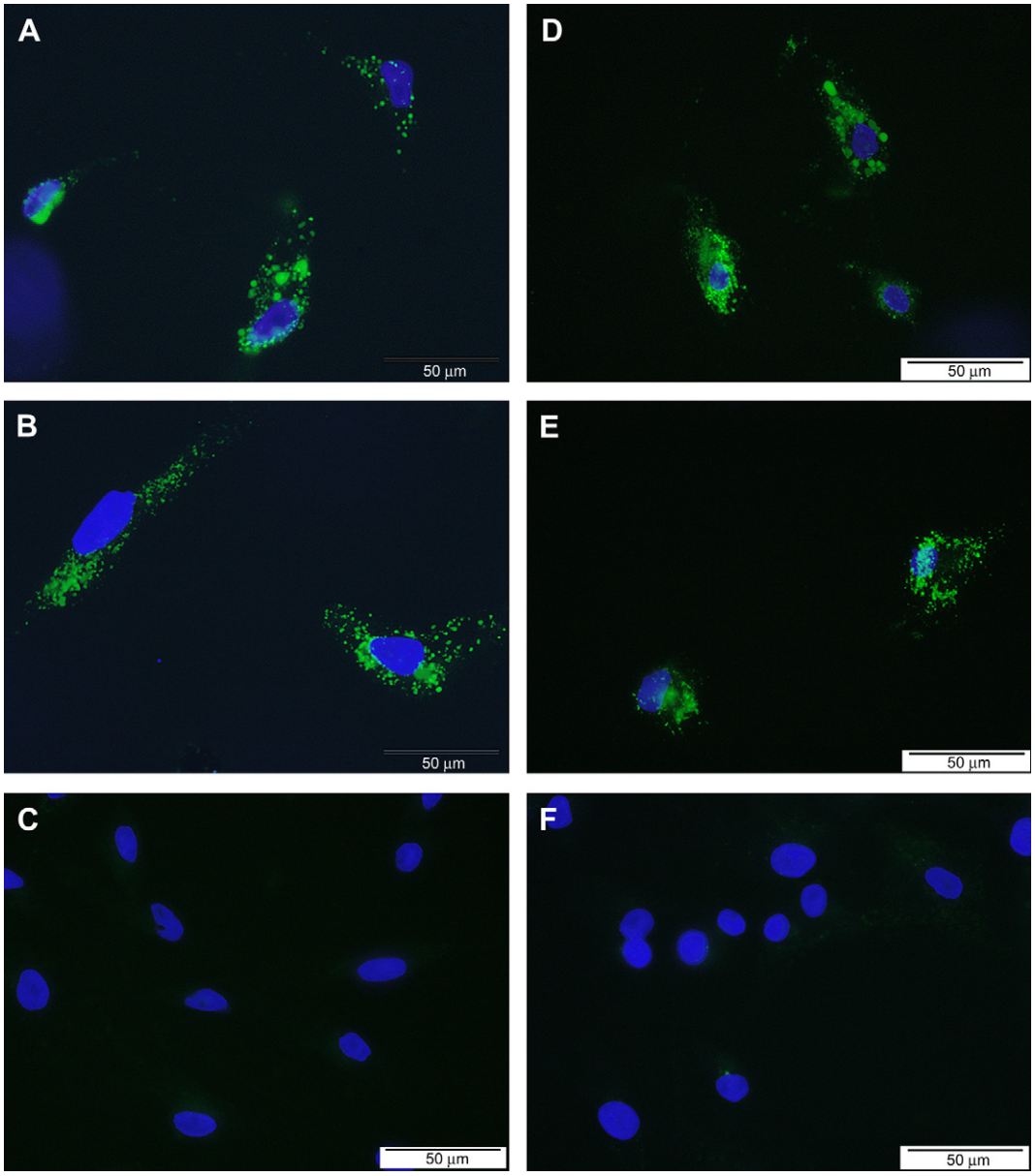

Fig. 8. Effects of CoCr nanoparticles on intra-cellular oxidative stress in porcine dural fibroblasts and dural epithelial cells. Particle-exposed fibroblasts (A, B, C) and epithelial cells (D, E, F) were treated with carboxy-H_2DCFDA and incubated at 37 °C for 25 min in the dark followed by counterstaining with the Hoechst stain for 5 min. Cells were washed thrice with PBS and immediately visualised using fluorescence microscopy at 400× magnification. The resulting oxidative stress was measured by evaluating the fluorescence intensity in 100 individual cells. (A, B, D, E) Strong or very strong fluorescence staining observed in cells treated with CoCr nanoparticles at a volume of 50 μm^3 per cell. (C, F) Relatively weak or no staining observed in the cells only negative control at the same particle dose. Note: Images may not be representative of the entire cell population.

agglomerated at different rates due to different protein content in the media. The CoCr particles sedimented at a slower rate in M199 medium (epithelial cells medium) compared to DMEM (fibroblasts medium), but both had fully sedimented by 6 h.

Similar to metal particles, the metal ions released from the CoCr nanoparticles had no significant effect on the viability of the dural fibroblasts. The metal ions significantly reduced the viability of the epithelial cells at day 3 and 4 of culture only at the highest dose (47.6 $\mu g \cdot ml^{-1}$ equivalent to 121 μm^3 per cell). There were however differences between the toxicity of CoCr nanoparticles and their ions for dural epithelial cells. The CoCr particles caused a reduction in cell viability at much lower volumetric doses (6.06, 60.6, 121 μm^3 per cell) and starting at a much earlier time point (day 2) relative to the metal ions (only at 47.6 $\mu g \cdot ml^{-1}$ equivalent to 121 μm^3 per cell, after day 3). These results suggested that extracellular ion release alone was not the cause of all the toxicity of the CoCr nanoparticles. This agreed with a study by Jiang *et al.* [52], who demonstrated that the cytotoxic as well as clastogenic effects of Co nanoparticles were much stronger than that of Co ions (equal concentrations).

Implant wear particles can stimulate chronic inflammatory and foreign body reactions mediated by proinflammatory cytokines and chemokines such as IL-1, IL-6, IL-8 and tumour necrosis factor-alpha (TNF-α) that can upregulate bone-resorbing osteoclasts [53,54], which may ultimately facilitate implant loosening. In preliminary tests, the dural-derived cells were treated with different cytokine-inducers such as phorbol-myristate acetate (PMA), phytohaemagglutinin (PHA), LPS, cholera toxin, cisplatin and calcium ionophore at different concentrations and at different combinations treatments. No significant release of IL-1, TNF-α or IL-6 was observed at many different time points suggesting that these cell types could not

Table 3
Classification of intra-cellular ROS signals in porcine dural fibroblasts and epithelial cells as an indicator of the extent of oxidative stress. Fluorescence intensity of individual cells was designated into four categories as shown. Intra-cellular ROS signals were evaluated after exposing the cells to CoCr nanoparticles for 24 h. Cells without treatment were used as the negative control. A total of 100 individual cells were counted and assigned various signal categories based on the observed intensity of the oxidised carboxy-DCF fluorescence. The number of cells in different categories is expressed in percentage.

	Dural fibroblasts		Dural epithelial cells	
	Cells (with CoCr)	Cells (negative control)	Cells (with CoCr)	Cells (negative control)
No signal (%)	0	72	0	64
Weak signal (%)	10	23	13	28
Strong signal (%)	40	5	25	8
Very strong signal (%)	50	0	62	0

be stimulated to release these cytokines. However, the only cytokine that was able to be induced was IL-8 (data not shown). IL-8 is an important chemotactic cytokine that is known to act as a potent attractant for neutrophils and lymphocytes [55]. Interestingly, IL-8 has also been found to play a pivotal role in the development of a delayed-type hypersensitivity reaction [56]. Based on these findings, it was thought prudent to investigate whether the dural fibroblasts and epithelial cells could act as a source of the pro-inflammatory chemokine IL-8 when cultured with CoCr nanoparticles up to 4 days. Both the fibroblasts and the epithelial cells were induced to secrete IL-8 upon treatment with the particles. The particles significantly increased the production of IL-8 from the fibroblasts at the highest dose of 121 μm^3 per cell at day 3 of culture only while the epithelial cells were consistently induced to secrete significantly higher levels of IL-8 at doses of 60.5 μm^3 and 121 μm^3 per cell after 1 day of culture with the particles. IL-8 has been shown to play a primary role in the early inflammatory response to CoCr wear particles [57,58]. Furthermore, Park *et al.* [59] have reported that an increase in oxidative stress can induce the up-regulation of IL-8 gene expression in human bronchial epithelial cells.

Metal wear particles have also been reported to induce the secretion of the proinflammatory cytokine IL-6 which can contribute to the maturation and activation of osteoclasts form osteoclast precursors, thereby leading to periprosthetic bone resorption [53,57]. Hence, the secretion of IL-6 was also examined. However, no significant release of IL-6 from the particle-exposed cells could be detected. These results are in agreement with a study by Papageorgiou *et al.* [21], where human skin fibroblasts treated with CoCr nano- and micro-particles did not stimulate any significant release of IL-6.

Increased oxidative stress has been observed in various cells cultured with CoCr nanoparticles [60]. Therefore, to analyse the potential of CoCr nanoparticles to generate ROS, both porcine dural fibroblasts and epithelial cells were treated with the particles at a dose of 50 μm^3 per cell which was found to be to cytotoxic only to the epithelial cells. CoCr nanoparticles were shown to have induced the generation of ROS in both cell types irrespective of their biological response to particle-induced toxicity, in agreement with previous findings [21]. Intriguingly, human endothelial cells have been demonstrated to be more susceptible to oxygen toxicity than fibroblasts, afforded by a lower content of anti-oxidant enzymes [61]. This finding may help explain the observed higher susceptibility of the dural epithelial cells to CoCr nanoparticle toxicity when compared to the dural fibroblasts.

Further *in vitro* studies would be required to expand the current knowledge about the biological effects of CoCr wear particles on the cellular milieu of the dura mater. Porcine dural fibroblasts and epithelial cells were shown to generate free radical species upon culture with CoCr nanoparticles. Hence, culturing particle-treated cells with oxygen radical scavengers [62] would help determine whether production of particle-induced ROS is responsible for the susceptibility of the dural epithelial cells to CoCr nanoparticle toxicity and also if ROS mediate IL-8 production in particle-treated cells. Secretion of IL-8 by dural cells in response to wear particles has not been reported previously. It is therefore proposed that CoCr nanoparticle-induced secretion of IL-8 by dural fibroblasts and epithelial cells may be involved in the pathophysiology associated with metal wear particles. Hence, it will be important to investigate the chemotactic activity of IL-8 secreted from particle-treated dural cells.

There appears to be a growing consensus in the scientific community that wear debris-mediated cytotoxicity, inflammatory responses and adverse tissue reactions may limit the clinical performance of orthopaedic metal implants. As such, prospective randomised clinical studies will be required to confirm the clinical relevance of the results obtained in this study. Study of explanted metal disc surfaces obtained during revision surgery using established techniques such as energy dispersive X-ray spectroscopy (EDS) and scanning electron microscopy (SEM) [63] may help in determining mechanisms of implant degradation. There has been remarkable progress in research aimed at resolving the biological effects of metal wear particles at the molecular and cellular levels. However, much needs to be done to completely understand such particle-initiated intricate biological mechanisms before any effective therapeutic interventions can be developed and made available in the clinical setting.

5. Conclusion

This study has demonstrated that porcine dural fibroblasts and epithelial cells differ in their response to CoCr nanoparticles and ions. Clinically relevant CoCr particulate wear debris at volumes of 6.05 μm^3, 60.5 μm^3 and 121 μm^3 per cell was shown to have significantly reduced the viability of the dural epithelial cells after 1 day of culture but not the dural fibroblasts. In addition, CoCr nanoparticles induced the secretion of IL-8 from the fibroblasts at a particle volume of 121 μm^3 per cell and from the epithelial cells at particle volumes of 60.5 μm^3 and 121 μm^3 per cell. Both cell types were also induced to generate reactive oxygen species when treated with the particles at a dose of 50 μm^3 per cell for 24 h. However, a difference in susceptibility of the two cell types to free radical species may explain the difference in their response to particle-induced toxicity. These findings may present an important step forward in understanding the complex biological factors involved in the adverse cellular responses to metal disc prostheses.

Acknowledgements

This work was supported by the National Institutes of Health grant R01-AR052653-01 and by the Leeds Centre of Excellence in Medical Engineering funded by the Wellcome Trust and EPSRC, WT088908/z/09/z. John Fisher is an NIHR senior investigator.

References

[1] Urban J, Roberts S. Degeneration of the intervertebral disc. Arthritis Res Ther 2003;5(3):120–30.
[2] Deyo RA, Nachemson A, Mirza SK. Spinal-fusion surgery - the case for restraint. N Engl J Med 2004;350(7):722–6.
[3] Kim BH, Choi DH, Jeon SH, Choi YS. Relationship between new osteoporotic vertebral fracture and instrumented lumbar arthrodesis. Asian Spine J 2010; 4(2):77–81.

[4] McGowan DP, Goel VK. Aching backs get support from FDA, but not payors. AAOS Now 2007;1(7):2007.
[5] Cunningham BW. Basic scientific considerations in total disc arthroplasty. Spine J 2004;4(6 Suppl):219S–30S.
[6] Le Huec JC, Mathews H, Basso Y, Aunoble S, Hoste D, Bley B, et al. Clinical results of Maverick lumbar total disc replacement: two-year prospective follow-up. Orthop Clin North Am 2005;36(3):315–22.
[7] Sasso RC, Foulk DM, Hahn M. Prospective, randomized trial of metal-on-metal artificial lumbar disc replacement: initial results for treatment of discogenic pain. Spine 2008;33(2):123–31.
[8] Anderson P, Rouleau J. Intervertebral disc arthroplasty. Spine 2004;29(23): 2779–86.
[9] Bao Q, Yuan H. Artificial disc technology. Neurosurg Focus 2000;9(4):e14.
[10] Villavicencio A, Burneikiene S, Johnson J. Spinal artificial disc replacement: lumbar arthroplasty: Part I. Contemp Neurosc 2005;27:1–5.
[11] Berry M, Peterson B, Alander D. A granulomatous mass surrounding a Maverick total disc replacement causing iliac vein occlusion and spinal stenosis: a case report. J Bone Jt Surg Am 2010;92(5):1242–5.
[12] Guyer RD, Shellock J, Maclennan B, Hanscom D, Knight RQ, McCombe P, et al. Early failure of metal-on-metal artificial disc prostheses associated with lymphocytic reaction: diagnosis and treatment experience in 4 Cases. Spine 2011;36(7):E492–7.
[13] Cabraja M, Schmeding M, Koch A, Podrabsky P, Kroppenstedt S. Delayed formation of a devastating granulomatous process after metal-on-metal lumbar disc arthroplasty. Spine 2012;37(13):E809–13.
[14] Doorn PF, Campbell PA, Worrall J, Benya PD, McKellop HA, Amstutz HC. Metal wear particle characterization from metal on metal total hip replacements: transmission electron microscopy study of periprosthetic tissues and isolated particles. J Biomed Mater Res 1998;42(1):103–11.
[15] Brown C, Williams S, Tipper JL, Fisher J, Ingham E. Characterisation of wear particles produced by metal on metal and ceramic on metal hip prostheses under standard and microseparation simulation. J Mater Sci Mater Med 2007; 18(5):819–27.
[16] Case CP, Langkamer VG, James C, Palmer MR, Kemp AJ, Heap PF, et al. Widespread dissemination of metal debris from implants. J Bone Jt Surg Br 1994;76(5):701–12.
[17] deSouza RM, Parsons NR, Dalton P, Costa M, Krikler S. Metal ion levels following resurfacing arthroplasty of the hip. J Bone Jt Surg Br 2010;92-B(12): 1642–7.
[18] Medicines and Healthcare products Regulatory Agency. Expert Advisory Group on 'Biological effects of metal wear debris generated from hip implants: genotoxicity" Report; 2010.
[19] Goodman SB. Wear particles, periprosthetic osteolysis and the immune system. Biomaterials 2007;28(34):5044–8.
[20] Huber M, Reinisch G, Trettenhahn G, Zweymüller K, Lintner F. Presence of corrosion products and hypersensitivity-associated reactions in periprosthetic tissue after aseptic loosening of total hip replacements with metal bearing surfaces. Acta Biomater 2009;5(1):172–80.
[21] Papageorgiou I, Brown C, Schins R, Singh S, Newson R, Davis S, et al. The effect of nano- and micron-sized particles of cobalt-chromium alloy on human fibroblasts *in vitro*. Biomaterials 2007;28(19):2946–58.
[22] Bhabra G, Sood A, Fisher B, Cartwright L, Saunders M, Evans W, et al. Nanoparticles can cause DNA damage across a cellular barrier. Nat Nanotechnol 2009;4(12):876–83.
[23] Service RF. Experts criticize nanoparticle study. ScienceNOW; 2009.
[24] Pandit H, Glyn-Jones S, McLardy-Smith P, Gundle R, Whitwell D, Gibbons CL, et al. Pseudotumours associated with metal-on-metal hip resurfacings. J Bone Jt Surg Br 2008;90(7):847–51.
[25] Zeh A, Planert M, Siegert G, Lattke P, Held A, Hein W. Release of cobalt and chromium ions into the serum following implantation of the metal-on-metal Maverick-type artificial lumbar disc. Spine 2007;32(3):348–52.
[26] Cavanaugh D, Nunley P, Kerr E, Werner D, Jawahar A. Delayed hypersensitivity to metal ions after cervical disc arthroplasty: a case report and literature review. Spine 2009;34(7):E262–5.
[27] Charnley J. Arthroplasty of the hip. a new operation. Lancet 1961;27;1(7187): 1129–32.
[28] Kurtz SM, Lau E, Ong K, Zhao K, Kelly M, Bozic KJ. Future young patient demand for primary and revision joint replacement: national projections from 2010 to 2030. Clin Orthop Relat Res 2009;467(10):2606–12.
[29] Burnett RSJ. Total hip arthroplasty: techniques and results. B C Mel J 2010; 52(9):455–64.
[30] Rosengren BE. Metal-on-metal hip implants and the risk of cancer. Br Med J 2012;345:e4605.
[31] Hallab NJ. A review of the biologic effects of spine implant debris: fact from fiction. SAS J 2009;3(4):143–60.
[32] Brown C, Fisher J, Ingham E. Biological effects of clinically relevant wear particles from metal-on-metal hip prostheses. Proc Inst Mech Eng H 2006; 220(2):355–69.
[33] Catelas I, Medley JB, Campbell PA, Huk OL, Bobyn JD. Comparison of *in vitro* with *in vivo* characteristics of wear particles from metal-metal hip implants. J Biomed Mater Res B Appl Biomater 2004;70(2):167–78.
[34] Chowdhury I, Hong Y, Walker SL. Container to characterization: impacts of metal oxide handling, preparation, and solution chemistry on particle stability. Colloids Surf A Physicochem Eng Asp 2010;368:91–5.
[35] Zhou D, Bennett SW, Keller AA. Increased mobility of metal oxide nanoparticles due to photo and thermal induced disagglomeration. PLoS ONE 2012;7(5):e37363.
[36] Mandzy N, Grulke E, Druffel T. Breakage of TiO2 agglomerates in electrostatically stabilized aqueous dispersions. Powder Techn 2005;160(2):121–6.
[37] Allouni ZE, Cimpan MR, Høl PJ, Skodvin T, Gjerdet NR. Agglomeration and sedimentation of TiO2 nanoparticles in cell culture medium. Colloids Surf B Biointerfaces 2009;68(1):83–7.
[38] Rezwan K, Meier LP, Gauckper LJ. Lysozyme and bovine serum albumin adsorption on uncoated silica and AlOOH-coated silica particles: the influence of positively and negatively charged oxide surface coatings. Biomaterials 2005;26(21):4351–7.
[39] Kuzmuk, Lawrence. Pigs as a model for biomedical sciences. In: Rothschild MF, Ruvinsky A, editors. The genetics of the pig. CABI Publishing; 2011. p. 426–44.
[40] Fairbairn L, Kapetanovic R, Sester DP, Hume DA. The mononuclear phagocyte system of the pig as a model for understanding human innate immunity and disease. J Leukoc Biol 2011;89(6):855–71.
[41] Lidington EA, Moyes DL, McCormack AM, Rose ML. A comparison of primary endothelial cells and endothelial cell lines for studies of immune interactions. Transpl Immunol 1999;7(4):239–46.
[42] Boerma M, Burton GR, Wang J, Fink LM, McGehee Jr RE, Hauer-Jensen M. Comparative expression profiling in primary and immortalized endothelial cells: changes in gene expression in response to hydroxy methylglutaryl-coenzyme: a reductase inhibition. Blood Coagul Fibrinolysis 2006;17(3): 173–80.
[43] Pan C, Kumar C, Bohl S, Klingmueller U, Mann M. Comparative proteomic phenotyping of cell lines and primary cells to assess preservation of cell type-specific functions. Mol Cell Proteomics 2009;8(3):443–50.
[44] Eriksson JE, DeChat T, Grin B, Helfand B, Mendez M, Pallari HM, et al. Introducing intermediate filaments: from discovery to disease. J Clin Invest 2009; 119(7):1763–71.
[45] Shiozaki H, Oka H, Inoue M, Tamura S, Monden M. E-cadherin mediated adhesion system in cancer cells. Cancer 1996;77(8 Suppl):1605–13.
[46] Green KJ, Jones JC. Desmosomes and hemidesmosomes: structure and function of molecular components. FASEB J 1996;10(8):871–81.
[47] Getsios S, Huen AC, Green KJ. Working out the strength and flexibility of desmosomes. Nat Rev Mol Cell Biol 2004;5(4):271–81.
[48] Olson AL, Pessin JE. Structure, function, and regulation of the mammalian facilitative glucose transporter gene family. Annu Rev Nutr 1996;16:235–56.
[49] Pusztaszeri MP, Seelentag W, Bosman FT. Immunohistochemical expression of endothelial markers CD31, CD34, von Willebrand Factor, and Fli-1 in normal human tissues. J Histochem Cytochem 2006;54(4):385–95.
[50] Keegan GM, Learmonth ID, Case CP. Orthopaedic metals and their potential toxicity in the arthroplasty patient - review of current knowledge and future strategies. J Bone Jt Surg Br 2007;89(5):567–73.
[51] Mahendra G, Pandit H, Kliskey K, Murray D, Gill HS, Athanasou N. Necrotic and inflammatory changes in metal-on-metal resurfacing hip arthroplasties. Acta Orthop 2009;80(6):653–9.
[52] Jiang H, Liu F, Yang H, Li Y. Effects of cobalt nanoparticles on human T cells in vitro. Biol Trace Elem Res 2012;146(1):23–9.
[53] Kwan TS, Padrines M, Théoleyre S, Heymann D, Fortun Y. IL-6, RANKL, TNF-alpha/IL-1: interrelations in bone resorption pathophysiology. Cytokine Growth Factor Rev 2004;15(1):49–60.
[54] Bendre MS, Montague DC, Peery T, Akel NS, Gaddy D, Suva LJ. Interleukin-8 stimulation of osteoclastogenesis and bone resorption is a mechanism for the increased osteolysis of metastatic bone disease. Bone 2003;33(1):28–37.
[55] Taub DD, Anver M, Oppenheim JJ, Longo DL, Murphy WJ. T lymphocyte recruitment by interleukin-8 (IL-8) - IL-8-induced degranulation of neutrophils releases potent chemoattractants for human T lymphocytes both in vitro and in vivo. J Clin Invest 1996;97(8):1931–41.
[56] Larsen CG, Thomsen MK, Gesser B, Thomsen PD, Deleuran BW, Nowak J, et al. The delayed-type hypersensitivity reaction is dependent on IL-8. Inhibition of a tuberculin skin reaction by an anti-IL-8 monoclonal antibody. J Immunol 1995;155(4):2151–7.
[57] Hallab N, Jacobs J. Biologic effects of implant debris. Bull NYU Hosp Jt Dis 2009;67(2):182–8.
[58] Kaufman AM, Alabre CI, Rubash HE, Shanbhag AS. Human macrophage response to UHMWPE, TiAlV, CoCr, and alumina particles: analysis of multiple cytokines using protein arrays. J Biomed Mater Res A 2008;84(2):464–74.
[59] Park EJ, Yi J, Chung YH, Ryu DY, Choi J, Park K. Oxidative stress and apoptosis induced by titanium dioxide nanoparticles in cultured BEAS-2B cells. Toxicol Lett 2008;180(3):222–9.
[60] Gill HS, Grammatopoulos G, Adshead S, Tsialogiannis E, Tsiridis E. Molecular and immune toxicity of CoCr nanoparticles in MoM hip arthroplasty. Trends Mol Med 2012;18(3):145–55.
[61] Michiels C, Toussaint O, Remacle J. Comparative-study of oxygen-toxicity in human fibroblasts and endothelial-cells. J Cell Physiol 1990;144(2): 295–302.
[62] DeForge LE, Fantone JC, Kenney JS, Remick DG. Oxygen radical scavengers selectively inhibit interleukin-8 production in human whole-blood. J Clin Invest 1992;90(5):2123–9.
[63] Kurtz SM, Steinbeck M, Ianuzzi A, Ooij Av, Punt IM, Isaza J, et al. Retrieval analysis of motion preserving spinal devices and periprosthetic tissues. SAS J 2009;3(4):161–77.